A three-dimensional Monte Carlo model for electrically conductive polymer matrix composites filled with curved fibers

H.M. Ma, X.-L. Gao*

Department of Mechanical Engineering, Texas A&M University, 3123 TAMU, College Station, TX 77843-3123, USA

ABSTRACT

A three-dimensional (3-D) Monte Carlo model is developed for predicting electrical conductivity of polymer matrix composites filled with conductive curved fibers. The conductive fillers are modeled as a 3-D network of finite sites that are randomly positioned. The percolation behavior of the network is studied using the Monte Carlo method, which leads to the determination of the critical fiber volume fraction (or the percolation threshold). The effect of fiber curliness on the percolation behavior is incorporated in the current model by using 3-D arm-shaped fibers, each of which needs five independent geometrical parameters (i.e., three coordinates for its vertex and two orientation angles) for its identification. There are three controlling parameters for such fibers, namely the fiber arm length, the fiber aspect ratio, and the fiber arm angle. The new model also considers the sample size and scaling effects. The simulation results reveal an exponential relationship between the fiber aspect ratio and the percolation threshold: the higher the aspect ratio, the lower the threshold. It is also found that the curliness largely influences the percolation threshold: the more curved the fiber, the higher the threshold. However, the effect of curliness diminishes with the increase of the fiber aspect ratio. With the percolation threshold obtained from the Monte Carlo model, the effective electrical conductivity of the composite is then determined by applying the theory of percolation. The numerical results indicate that the composite conductivity decreases as the fibers become more curved and as the fiber aspect ratio decreases. These predicted trends of the percolation threshold and composite conductivity are in good agreement with existing experimental and simulation results.

1. Introduction

Electrically conductive polymer matrix composites (PMCs) filled with conductive particles or fibers are finding important applications in aerospace and other industries. For example, PMCs reinforced by nickel nanostrands, which are pure nickel filaments with nanometer diameters and high aspect ratios, are very promising nanocomposites that can reduce lightning strike damage with minimum added weight [15,19]. Experimental studies have revealed the existence of an insulator-to-conductor transition in such a composite around a critical threshold as the volume fraction of conductive fillers (ϕ) increases [5]. That is, there is a sharp onset of high electrical conductivity (σ) at a critical fiber volume fraction (ϕ_c) (see Fig. 1).

Percolation theory has been widely used to describe this transition [14,27,11]. In the theory of site percolation, conductive fillers

in a composite are modeled as a two-dimensional (2-D) or three-dimensional (3-D) network of sites, which are regularly or randomly located in the composite system. The connection between each two neighboring sites may be open (allowing the current through) with probability p, or closed with probability $1 - p$. It has been found that there exists a critical probability p_c (a threshold value) above which a continuous pathway will always be present in the system. Studies on electrical conductivity of composites have been mainly focused on investigating the percolation threshold in order to understand the sharp change in conductivity near the insulator–conductor transition [21,7]. Exact solutions to percolation problems have been obtained only for a few special cases [10,22], while approximate approaches, such as the Monte Carlo method, are necessitated for other cases.

In the Monte Carlo method, the topological disorder in a random microstructure is directly captured, and the percolation behavior is effectively simulated using advanced computational algorithms. The earliest use of the Monte Carlo method in solving percolation problems was made by Pike and Seager [27], who carried out a 2-D study on composites filled by straight sticks. In

* Corresponding author. Tel.: +1 979 845 4835.
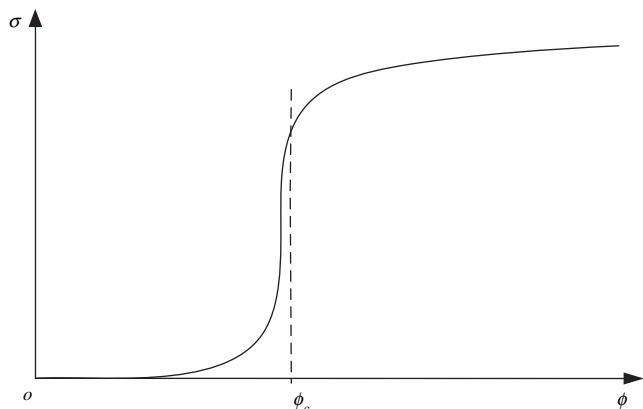 E-mail address: xlgao@tamu.edu (X.-L. Gao).

Fig. 1. Conductivity depending on the filler volume fraction.

their work, the sticks were assumed to be of equal length but no width. Balberg and Binenbaum [2] extended Pike and Seager's work by accounting for the macroscopic anisotropy induced by sticks with preferred orientation and/or unequal length. More recently, the width of sticks was taken into consideration by Natsuki et al. [23] in their Monte Carlo simulation of 2-D stick (short-fiber) networks, where the dependence of the percolation threshold on the fiber aspect ratio and orientation angle was studied.

The Monte Carlo method has also been used to investigate 3-D percolation problems. The first 3-D Monte Carlo study on percolation behavior of systems consisting of randomly oriented sticks (capped cylinders) in the 3-D space was conducted by Balberg et al. [4], in which the effects of the stick aspect ratio and macroscopic anisotropy were explored. The in-plane electrical conductivity of a 3-D composite reinforced by straight short fibers was studied by Taya and Ueda [29] using the Monte Carlo approach developed in Balberg et al. [4] and an effective medium method. The 3-D Monte Carlo simulations by Lee and Kim [16] were performed for unidirectional short-fiber reinforced composites, where the fiber orientation was predetermined and only the fiber aspect ratio, fiber volume fraction and fiber length distribution were allowed to change. Clearly, the last two studies reviewed above did not account for the full randomness of 3-D composite systems due to the restrictive conditions employed by the authors. In addition, these and most of other works on percolation behavior of composites have been confined to composites filled with straight fibers. Since some filler materials such as nickel nanostrands used to fabricate conductive polymer matrix composites are highly flexible due to their very large aspect ratios [15,19], the conductivity of such a composite system will certainly be different from that of a composite embedded with only straight fibers.

Very limited attention has been paid to the effects of fiber curliness and entanglement on the percolation behavior of fibrous composites. It has been reported by Yi et al. [31] that the percolation threshold significantly increases with increasing waviness of sinusoid-shaped fibers. Very recently, a general continuum percolation model was developed by Li and Chou [18] for composites filled with curved fibers of arbitrary shape. But these two studies were devoted to 2-D fiber networks. Dalmas et al. [8] simulated 3-D entangled fibrous networks using spline-shaped fibers. They found that increasing fiber tortuosity leads to an increased percolation threshold and the effect of the fiber tortuosity is larger if the fiber aspect ratio is higher. However, the effect of the fiber width (nanotube diameter) was not explicitly studied in their 3-D simulations. Therefore, there is still a need to develop 3-D Monte Carlo models that account for the effects of fiber aspect ratio, fiber curliness and fiber width on the percolation behavior of composites.

The objective of this paper is to provide such a percolation model by using randomly distributed and oriented 3-D arm-shaped fibers, which provide a first approximation to actual, curved filler materials such as nickel nanostrands. The rest of the paper is organized as follows. In Section 2, the 3-D Monte Carlo model is formulated analytically. Sample numerical results are presented in Section 3 to illustrate the newly developed model. A summary is provided in the fourth and last section.

2. Formulation

Two steps are involved in developing the Monte Carlo model presented here. In the first step, arm-shaped fibers with randomly located vertices and random orientations are generated. Since the main objective of this study is to determine the filler volume fraction at the onset of high electrical conductivity, a non-dimensionalized unit cube will be used, as was done in other studies on percolation problems [4,23]. In the second step, a bonding (connection) criterion is applied to check the connectivity between each pair of fibers in the cube (composite system). The connected fibers will form a continuous cluster and may lead to a pathway. The details of these two steps are described below.

2.1. Model generation

To generate the composite system with randomly distributed fibers, the sites, as the vertices of arm-shaped fibers, are first placed inside a unit cube using their coordinates that are randomly generated (see below). Then, each site is attached with an arm-shaped fiber having two arms separated by angle γ, as shown in Fig. 2. The two arms are assumed to have the same length L and diameter D. Another three independent angles, α_1^i, α_2^i and θ_1^i (see Fig. 3), which are needed to determine the orientation of the ith 3-D arm-shaped fiber, are also generated randomly (see below). All the arm-shaped fibers in the system are taken to be identical (i.e., having the same arm length, diameter and arm angle). But they are randomly distributed and oriented. With γ being adjustable, the 3-D arm-shaped fiber model proposed here is expected to provide a good first approximation to curved fibers.

To generate numbers with sufficient randomness, the multiplicative congruential (MC) generator is adopted, which is the most common computer technique for producing random sequences [1]. The implementation details of this generator can be found in Park
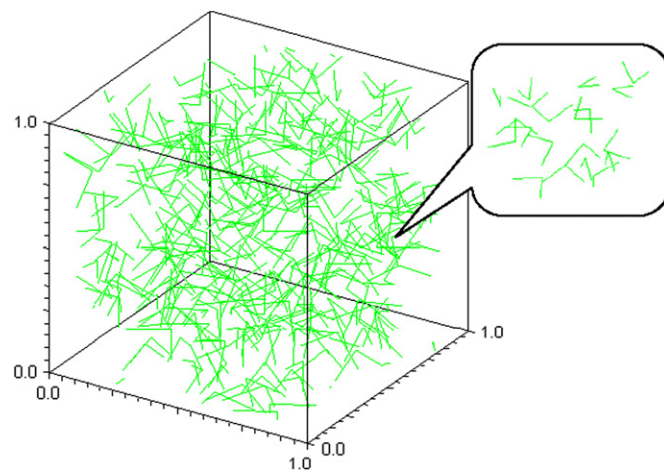

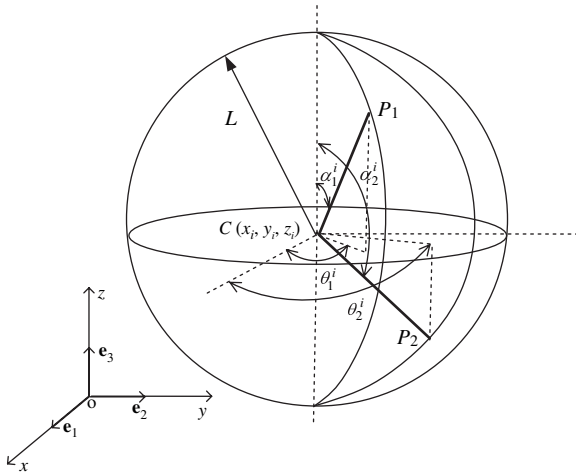Fig. 2. System with randomly distributed arm-shaped fibers.

Fig. 3. Position of an arm-shaped fiber.

and Miller [26]. To avoid the patterned lattice effect, which can arise when long runs (such as 5000 numbers long) are generated by the MC generator and can undermine the randomness of the sequences [1], the MC generator is called once to generate all information needed to identify an arm-shaped fiber (i.e., three coordinates for the fiber vertex and three independent angles, α_1^i, α_2^i and θ_1^i, for the fiber orientation of the ith fiber, as will be discussed below). That is, six random numbers ranging from 0 to 1 are generated by using the MC generator once. The site coordinates are given by the first three random numbers, while the orientation angles are obtained from the other three random numbers. As an example, a resulting system with 400 randomly distributed and oriented arm-shaped fibers is shown in Fig. 2.

2.2. Connection criterion

For an arm-shaped fiber in the system, the coordinates (x, y, z) of any point on the axis of the ith fiber whose vertex (central point) is located at $C(x_i, y_i, z_i)$ can be represented by (see Fig. 3)

$$\begin{Bmatrix} x \\ y \\ z \end{Bmatrix} = \begin{Bmatrix} x_i \\ y_i \\ z_i \end{Bmatrix} + t \begin{Bmatrix} \cos\theta_1^i \sin\alpha_1^i \\ \sin\theta_1^i \sin\alpha_1^i \\ \cos\alpha_1^i \end{Bmatrix} \text{ or}$$

$$\begin{Bmatrix} x \\ y \\ z \end{Bmatrix} = \begin{Bmatrix} x_i \\ y_i \\ z_i \end{Bmatrix} + t \begin{Bmatrix} \cos\theta_2^i \sin\alpha_2^i \\ \sin\theta_2^i \sin\alpha_2^i \\ \cos\alpha_2^i \end{Bmatrix} \quad \text{(no sum on } i) \quad (1)$$

where $t(\in[0, L])$ is the distance from C to the point of interest, α_1^i $(\in[0,180°])$, θ_1^i $(\in[0, 360°])$ are the orientation angles for one arm, and α_2^i $(\in[0,180°])$, θ_2^i $(\in[0,360°])$ are the orientation angles for the other arm. There is a constraint among these four orientation angles, since the angle between the two arms is predetermined. The constraint is (see Fig. 4)

$$d = 2L \sin\frac{\gamma}{2}, \quad (2)$$

where d is the distance between the two centers of the end sections of the arm-shaped fiber whose coordinates are given by Eq. (1) with $t = L$. That is,
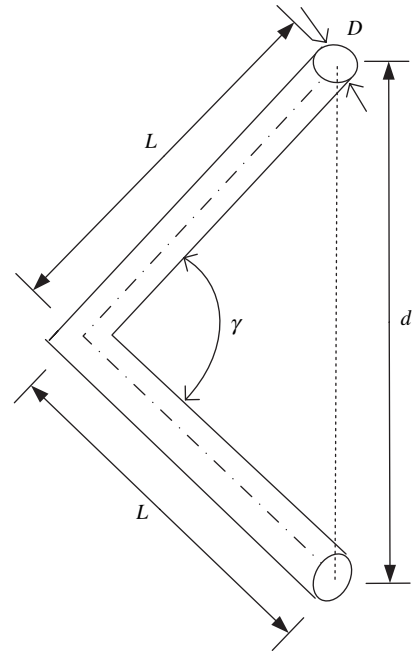

Fig. 4. Shape of an arm-shaped fiber.

Using Eq. (3) in Eq. (2) then yields, after simplifying,

$$1 - \cos\alpha_1^i \cos\alpha_2^i - \cos\left(\theta_1^i - \theta_2^i\right)\sin\alpha_1^i \sin\alpha_2^i = 2\left(\sin\frac{\gamma}{2}\right)^2 \quad (4)$$

as the constraint. Accordingly, only three of the four orientation angles are independent. Here α_1^i, α_2^i and θ_1^i are chosen to be the three independent orientation angles for the ith fiber with the vertex (x_i, y_i, z_i), whose values will be produced using the random number generator MC mentioned earlier. The value of θ_2^i can then be determined from Eq. (4).

Percolation occurs in the composite system if a continuous conducting pathway along any one or all of the three coordinate axes can be identified. To evaluate the status of the system generated above, each fiber in the system is checked against another to see whether they intersect. In the current study, the connectivity between the ith and jth fibers is determined by comparing the shortest distance between their axes with the fiber diameter.

Similar to those equations given in Eq. (1) for the ith fiber, the equations for the axis of the jth arm-shaped fiber in the system can be expressed in a vector-parametric form as

$$\begin{Bmatrix} x \\ y \\ z \end{Bmatrix} = \begin{Bmatrix} x_j \\ y_j \\ z_j \end{Bmatrix} + s \begin{Bmatrix} \cos\theta_n^j \sin\alpha_n^j \\ \sin\theta_n^j \sin\alpha_n^j \\ \cos\alpha_n^j \end{Bmatrix}$$

$$(n = 1, 2; \text{ no sum on } j \text{ or } n), \quad (5)$$

where $s(\in[0, L])$ is the distance from the central point of the jth fiber. The square of the distance between any two points respectively on the axes of the ith and jth fibers, F, can then be obtained from Eqs. (1) and (5) as

$$F = \mathbf{u} \cdot \mathbf{u}, \quad (6)$$

$$d = L\sqrt{\left(\cos\theta_1^i \sin\alpha_1^i - \cos\theta_2^i \sin\alpha_2^i\right)^2 + \left(\sin\theta_1^i \sin\alpha_1^i - \sin\theta_2^i \sin\alpha_2^i\right)^2 + \left(\cos\alpha_1^i - \cos\alpha_2^i\right)^2}. \quad (3)$$

where

$$\mathbf{u} = \left(x_i - x_j + t \cos \theta_m^i \sin \alpha_m^i - s \cos \theta_n^j \sin \alpha_n^j\right)\mathbf{e}_1$$
$$+ \left(y_i - y_j + t \sin \theta_m^i \sin \alpha_m^i - s \sin \theta_n^j \sin \alpha_n^j\right)\mathbf{e}_2$$
$$+ \left(z_i - z_j + t \cos \alpha_m^i - s \cos \alpha_n^j\right)\mathbf{e}_3 \quad (m = 1, 2;$$
$$n = 1, 2; \text{no sum on } m \text{ or } n) \tag{7}$$

is the distance vector between the two points (see Fig. 5), with $\mathbf{e}_i$ ($i = 1, 2, 3$) being the unit base vectors for the Cartesian coordinate system shown in Fig. 3.

$$d_{\min} = \begin{cases} \left(\dfrac{C_2^2 C_4 + C_1^2 + C_3^2 - C_1 C_2 C_3 - 4C_4}{C_2^2 - 4}\right)^{1/2} & \text{when } t = t_0, s = s_0, \text{ if } \alpha_m^i \neq \alpha_n^j, \theta_m^i \neq \theta_n^j; \\ \left(C_4 - \dfrac{C_1^2}{4}\right)^{1/2} & \text{when } s - t = \dfrac{C_1}{2}, \text{ if } \alpha_m^i = \alpha_n^j, \theta_m^i = \theta_n^j. \end{cases} \tag{14}$$

Using Eq. (7) in Eq. (6) then gives

$$F = t^2 + C_1 t + C_2 ts + s^2 + C_3 s + C_4, \tag{8}$$

where

$$\left.\begin{aligned} C_1 &= 2\Delta x \cos \theta_m^i \sin \alpha_m^i + 2\Delta y \sin \theta_m^i \sin \alpha_m^i + 2\Delta z \cos \alpha_m^i, \\ C_2 &= -2\left[\sin \alpha_m^i \sin \alpha_n^j \cos\left(\theta_m^i - \theta_n^j\right) + \cos \alpha_m^i \cos \alpha_n^j\right], \\ C_3 &= -2\Delta x \cos \theta_n^j \sin \alpha_n^j - 2\Delta y \sin \theta_n^j \sin \alpha_n^j - 2\Delta z \cos \alpha_n^j, \\ C_4 &= (\Delta x)^2 + (\Delta y)^2 + (\Delta z)^2, \\ \Delta x &= x_i - x_j, \Delta y = y_i - y_j, \Delta z = z_i - z_j. \end{aligned}\right\} \tag{9}$$

From Eq. (8), it is seen that F is a function of two variables, s and t. To find the minimum value of F, it is necessary that, using Eq. (8),

$$\frac{\partial F}{\partial t} = 2t + C_1 + C_2 s = 0, \quad \frac{\partial F}{\partial s} = 2s + C_3 + C_2 t = 0. \tag{10a,b}$$

Solving Eq. (10a,b) simultaneously gives

$$t_0 = \frac{2C_1 - C_2 C_3}{C_2^2 - 4}, \quad s_0 = \frac{2C_3 - C_1 C_2}{C_2^2 - 4}, \tag{11}$$

which defines the critical point (t_0, s_0) of $F(t, s)$. For $F(t_0, s_0)$ to be the minimum of $F(t, s)$, it is further required that

$$\frac{\partial^2 F}{\partial t^2} > 0, \quad \left(\frac{\partial^2 F}{\partial t^2}\right)\left(\frac{\partial^2 F}{\partial s^2}\right) - \left(\frac{\partial^2 F}{\partial t \partial s}\right)^2 > 0. \tag{12}$$
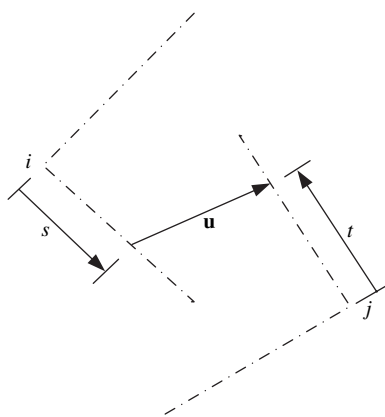
Fig. 5. Distance between the axes of the ith and jth fibers.

From Eq. (8) it follows that

$$\frac{\partial^2 F}{\partial t^2} = 2 > 0, \quad \left(\frac{\partial^2 F}{\partial t^2}\right)\left(\frac{\partial^2 F}{\partial s^2}\right) - \left(\frac{\partial^2 F}{\partial t \partial s}\right)^2 = 4 - C_2^2 > 0. \tag{13a,b}$$

Eq. (13b) holds as long as the two fibers are not parallel to each other (i.e., $\alpha_m^i \neq \alpha_n^j, \theta_m^i \neq \theta_n^j$) (see Appendix A for a proof). Eq. (13a,b) indicate that the conditions listed in Eq. (12) are satisfied by any pair of (t, s) involved in Eq. (8) for two fibers that are not parallel. Hence, F does have the minimum value when $t = t_0$ and $s = s_0$.

Substituting Eq. (11) into Eq. (8) gives the minimum distance between the axes of the ith and jth fibers as

If $d_{\min} \leq D$ with $0 \leq t_0 \leq L$ and $0 \leq s_0 \leq L$, then the ith and jth fibers are considered as connected. This type of connection is called the body-to-body connection (see Fig. 6(a)). Note that this connection criterion has also been used in other existing percolation models [24,23]. Meeting the criterion of $d_{\min} \leq D$ by each pair of fibers will certainly result in a continuous conducting network. Hence, this criterion can be viewed as a sufficient condition for forming a conductive pathway, while it may not be a necessary condition because of the existence of the tunneling effect. Indeed, tunneling between isolated fibers can be important, since it might take place before the percolation threshold is reached and could significantly contribute to the electrical conduction of a polymer matrix composite filled with conductive fibers [20,30], which is in addition to the conduction due to percolation in a continuous conducting network formed by connected fibers. Fortunately, it has been found [30] that a tunneling (non-continuous conducting) network, which is electrically connected but geometrically separated, existing in a composite can also be well described using the percolation theory for two-phase composites filled by conductive fibers that form a continuous conducting network. Hence, the tunneling effect will not be treated separately in the current study, and the above-mentioned connection criterion will be applied in all cases.

There are two other connection patterns in which two fibers do not satisfy the above condition but are still connected. These are known as the end-to-end and end-to-body connections [24], as shown in Fig. 6(b) and (c), respectively. In the end-to-end connection, where $t_0 > L$ and $s_0 > L$, the connection criterion is that the distance between the centers of the end circles of two fibers is not larger than D (see Fig. 6(b)). Similarly, in the end-to-body connection, where $t_0 > L$ or $s_0 > L$, two fibers are regarded as connected if the distance between the center of the end circle of one
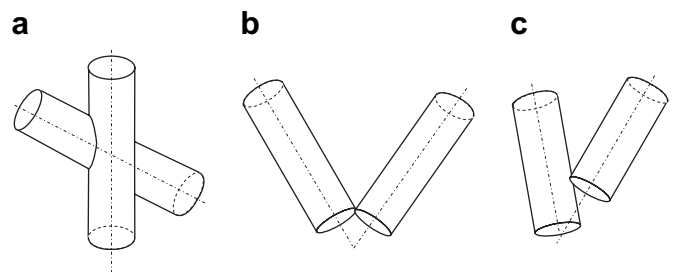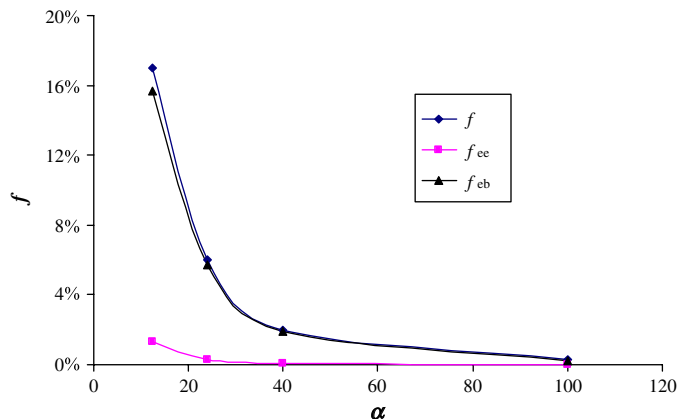
Fig. 6. Three patterns of fiber connections. (a) Body-to-body. (b) End-to-end. (c) End-to-body.

Fig. 7. Comparison of the fractions of the end-to-end (f_{ee}), end-to-body (f_{eb}), and total end ($f = f_{ee} + f_{eb}$) connections, with the fraction of the body-to-body connection being $1 - f$.

cluster 1 — — — — ·

Fig. 8. A cluster (continuous pathway) in the system.

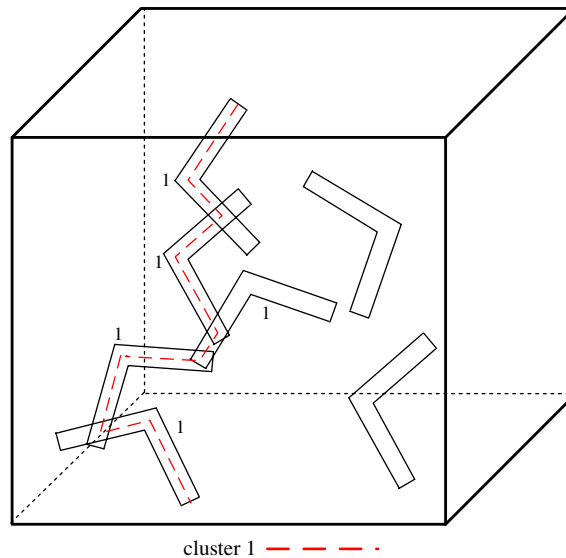fiber and the central line of another fiber is not larger than D (see Fig. 6(c)).

As discussed above and shown in Fig. 6, $d_{min} \leq D$ is only the necessary condition for all three patterns (i.e., body-to-body, end-to-end, and end-to-body) of connection. The connectivity of two fibers also depends on the values of t_0 and s_0 relative to L. In addition, if the point of intersection of two fibers is outside the sample (cube), then the two fibers are not considered as connected even if $0 \leq t_0 \leq L$ and $0 \leq s_0 \leq L$.

The end-to-end and end-to-body connecting patterns are more time consuming to model than the body-to-body connection in the Monte Carlo simulations because of the open ranges for t_0 and/or s_0 (i.e., $t_0 > L$ and/or $s_0 > L$ for the former as opposed to $0 \leq t_0 \leq L$ and $0 \leq s_0 \leq L$ for the latter). The fraction of the number of these two types of connections to the number of total connections among all fibers in the system is examined. It is found that this fraction drastically decreases with the increase of the fiber aspect ratio, as shown in Fig. 7. It is about 6% as the fiber aspect ratio reaches 24. Simulations incorporating the two end connections and the ones without them are performed for fibers having an aspect ratio of 24. The difference in the critical fiber volume fraction between these two sets of simulation results is found to be negligibly small (less than 2%). Therefore, for the sake of computational efficiency, the effects of the end-to-end and end-to-body connections are neglected for fibers with an aspect ratio greater than 24.

2.3. Computational implementation

Each fiber is assigned a fiber number and a cluster number when the generation procedure is completed. The fiber number and the cluster number are equal and range from 1 through N, where N is the total number of arm-shaped fibers in the system. Then, each fiber is checked for connection with other fibers whose fiber numbers are larger than its fiber number. For example, the ith fiber will be checked against the $(i + 1)$th through the Nth fibers. If two fibers satisfy the connection criterion, they will be assigned a common cluster number which is the smaller one of the two fiber numbers. As a result, all fibers within the same cluster have the same cluster number, and two clusters are given the same cluster number if they have a common fiber.

If any two fibers in opposite boundary regions have the same cluster number, then it can be concluded that the system is percolated in the direction perpendicular to the two opposing bounding surfaces [27]. For example, a percolating cluster along the vertical direction is clearly seen for the system schematically shown in Fig. 8. When the first percolating cluster is found, the system is said to be in the critical state where the critical fiber volume fraction has been reached.

3. Results and discussion

In the new percolation model developed in the preceding section, there are three controlling parameters for a given system (a unit cube): the fiber arm length L, the fiber aspect ratio α, and the fiber arm angle γ, which are all predetermined. The percolation threshold depends on these specified parameters.

For a given set of the values of the three controlling parameters, the number of fibers in the system, N, will be increased in small increments (with the random number generator reset for each increment) until the first cluster connecting the top and bottom surfaces of the cube is identified, which corresponds to one critical value of the fiber volume fraction.

3.1. Sample size effect

The sample size must be adequately specified in order to obtain accurate results. To determine the adequate sample size, the averages and the standard deviations of the critical fiber number (N_c) for sampling with 5, 10, 15, 20, 30, 40, 50 units, respectively, are obtained and shown in Fig. 9. Note that N_c is directly related to the critical fiber volume fraction ϕ_c through $\phi_c = \pi D^2 L N_c / 2$. For all of the cases illustrated in Fig. 9, the fiber arm length and arm angle are, respectively, fixed to be $L = 0.12$ and $\gamma = 180°$, and the fiber aspect ratio α, which is defined to be $2L/D$, is taken to be 24.

It is seen from Fig. 9 that the averages and the deviations tend to stabilize as the sampling units become greater than 15. This indicates that the best computational efficiency is achieved when the sample size is 15. For the cases with $\alpha = 12.5$ and 100, respectively, similar statistical analyses are performed, which leads to the same conclusion. Therefore, a sample containing 15 sampling units is selected for all simulations. Furthermore, the initial fiber number is adjusted so that the standard deviations of the results in all simulations are less than 5%.

3.2. Scaling effect

The finite-size effect is an issue that has to be addressed in all Monte Carlo simulations [28]. The percolation threshold, by definition, is the critical fiber volume fraction at which an infinitely
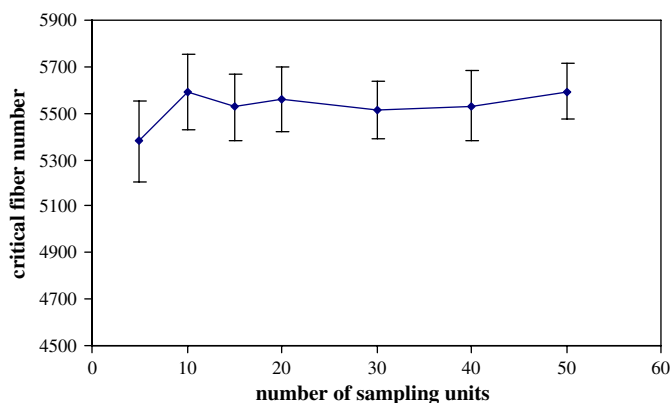
Fig. 9. Effect of the sample size on the critical volume fraction.

Fig. 10. Critical fiber volume fraction varying with the fiber length (with $\alpha = 24$).

large cluster of connecting fibers is found in an infinite composite system [28]. However, simulated systems are always finite. Therefore, percolation thresholds obtained from Monte Carlo simulations of finite systems need to be extrapolated before they can be used to predict asymptotic thresholds of infinitely large systems.

Following Stauffer [28], the relationship between the percolation threshold for a finite-size system, P_C, and that for an infinitely large system, P_∞, can be written as

$$P_C - P_\infty \propto C^{-1/\nu}, \tag{15}$$

where C is a characteristic size of the system being simulated, and ν is a correlation length exponent.

As mentioned earlier, the simulation box is a cube having a non-dimensional unit side length (i.e., $x \in [0, 1], y \in [0, 1], z \in [0, 1]$ in the system), and the size of each fiber in the simulated system is non-dimensionalized by the system size. Thus, the fiber arm length L is inversely proportional to the system size represented by C, and Eq. (15) becomes

$$P_C - P_\infty \propto L^{1/\nu}. \tag{16}$$

Based on Eq. (16), extrapolating the results obtained for a finite system with varying fiber arm length will lead to the threshold for the infinitely large system. Levinshtein et al. [17] conducted thousands of simulations for variously sized lattices to obtain $\nu = 0.9 \pm 0.05$ for 3-D lattices. Boissonade et al. [6] found $\nu = 0.875 \pm 0.03$ based on their Monte Carlo simulations of 3-D lattices. Dani and Ogale [9] concluded that $\nu = 0.89$ by using their model for cylindrical fibers. Based on these studies, ν is taken to be 0.9 in the current analysis. Then, Eq. (16) becomes

$$P_C - P_\infty \propto L^{1/0.9}. \tag{17}$$

To compare with existing experimental results of Bigg [5] for composites filled with straight fibers, the fiber arm angle, γ, is set to be 180°. The fiber aspect ratio, α ($= 2L/D$), is, respectively, taken to be 24 and 12.5, which is the same as that used in Bigg [5]. The third controlling parameter, the arm length L, is allowed to have different values. The Monte Carlo simulations are then conducted for the values of the controlling parameters identified above, and the simulation results of the critical fiber volume fraction (ϕ_c) versus the fiber arm length (L) are displayed in Figs. 10 and 11 for the two fixed values of $\alpha = 24$ and 12.5, respectively. For each of these two cases, it is seen from Figs. 10 and 11 that the discrete numerical results can be fitted as a straight line, indicating ϕ_c as a linear function of $L^{1/0.9}$. By extrapolating the straight line to the vertical axis, where the length of the fiber approaches zero or the system size goes to infinity, the intercept gives the critical fiber volume fraction for the infinitely large system as 8.0% and 16.5%,
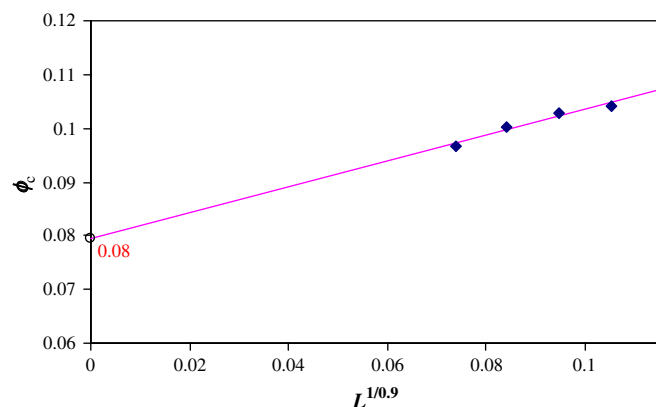
respectively, for $\alpha = 24$ and 12.5, as shown in Figs. 10 and 11. This compares fairly well with Bigg's experimental results of 6% for $\alpha = 24$ and 11% for $\alpha = 12.5$, considering the approximate nature of the Monte Carlo simulations and the possible scattering of the above-mentioned experimental data. The latter were given as two single values (rather than as averages and deviations or error bars) in Bigg [5] using aluminum fiber filled polymer (polypropylene) matrix composite specimens of finite dimensions.

3.3. Fiber aspect ratio effect

The effect of the aspect ratio on the percolation threshold is very important. It is found in the experimental study of Bigg [5] that for 3-D composites reinforced by straight short fibers the critical fiber volume fraction is strongly dependent on this parameter. The higher the fiber aspect ratio is, the lower the critical fiber volume fraction is required to induce electrical conductivity. It was revealed in the 2-D Monte Carlo study of Natsuki et al. [23] that the percolation threshold has a linear dependence on the fiber aspect ratio in a log–log plot when the aspect ratio is greater than 40.

In the current study, the effects of the fiber curliness and aspect ratio are investigated separately. A straight fiber is first simulated to exclude the effect of the fiber shape. The results for straight fibers (i.e., $\gamma = 180°$) with α increasing from 12.5 to 100 are listed in Table 1 and illustrated in Fig. 12, where the scaling effect discussed in Section 3.2 has been eliminated.

From Fig. 12, it is seen that a linear relationship exists between $\ln \alpha$ and $\ln(\phi_c)$. The slope of the straight line in Fig. 12, k, found through curve fitting is -1.14, which means that ϕ_c is proportional to $\alpha^{-1.14}$. That is, ϕ_c decreases exponentially with the increase of α, as was experimentally observed by Bigg [5]. The exponential
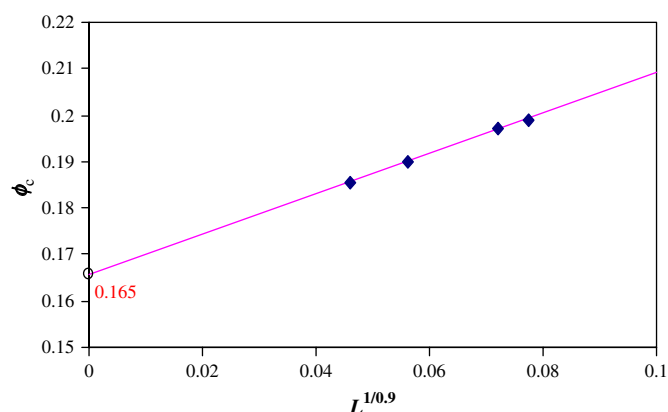

Fig. 11. Critical fiber volume fraction varying with the fiber length (with $\alpha = 12.5$).

Table 1
ϕ_c for straight fibers with various values of α

α	ϕ_c (%)	α	ϕ_c (%)
12.5	16.5	50	4.0
20	11.2	60	3.0
24	8.0	80	2.0
40	5.3	100	1.6

relation found here also agrees with that reported by Foygel et al. [12], which showed that $\phi_c \propto \alpha^{-1.0}$ (see their Fig. 4) for carbon nanotube reinforced composites.
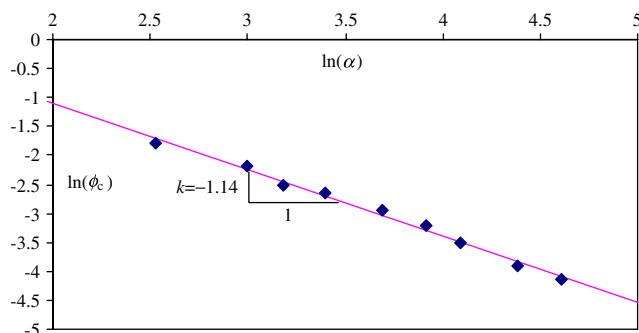
3.4. Fiber arm angle effect

The curliness of fibers has a great influence on the percolation threshold, as was shown by Yi et al. [31] in their study involving 2-D curly fibers of sinusoidal, triangular and rectangular shapes. In the current study, the fiber arm angle, γ (see Fig. 4), is used to represent the curliness of the fiber. The closer to 180° the arm angle is, the more the fiber is like a straight fiber, and hence the smaller the fiber curliness is. The fiber reaches its largest curliness when the arm angle approaches 0.

The simulation results for fibers with aspect ratios of 12.5, 24, 50 and 100 are plotted in Fig. 13, where the scaling effect discussed in Section 3.2 has already been eliminated. Fig. 13 shows that for all these four types of fibers, the critical fiber volume fraction decreases as the arm angle increases (i.e., as the fiber becomes less curved). It is also seen that the critical fiber volume fraction curves get more flat when the aspect ratio increases. For $\alpha = 50$, the $\phi_c(\gamma)$ curve is almost flat. This indicates that the effect of the fiber curliness on the critical fiber volume fraction is more significant for fibers with lower aspect ratios. When the aspect ratio is greater than 50, the $\phi_c(\gamma)$ curve is seen to be even more flat (see Fig. 13 for the case with $\alpha = 100$). That is, the critical volume fraction becomes virtually independent of the fiber curliness when $\alpha \geq 50$ for the system considered.

The logarithmic relations of the critical fiber volume fraction versus the fiber aspect ratio are plotted in Fig. 14 for fibers with an arm angle of 30°, 90°, 180°, respectively. The straight lines in Fig. 14 are seen to fit well with the data for different types of fibers, which means that the exponential relation between the critical fiber volume fraction and the aspect ratio observed for the straight fibers (with $\gamma = 180°$) in Section 3.3 and from Fig. 14 also holds for all of the curved fibers considered. That is, the critical fiber volume fraction decreases exponentially with increasing fiber aspect ratio for the fibers with different curliness.

3.5. Electrical conductivity

According to the percolation theory [14,3,28,25,13,19], the effective electrical conductivity of a composite, σ_e, can be obtained as
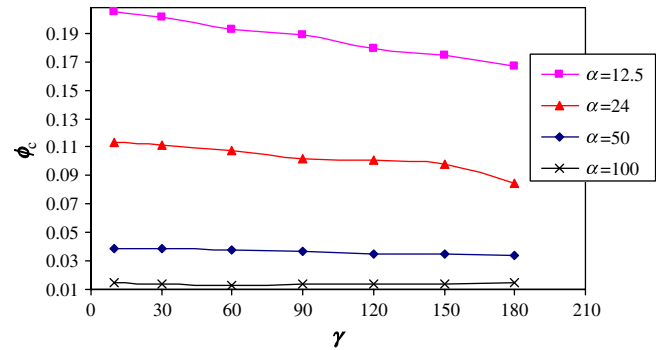
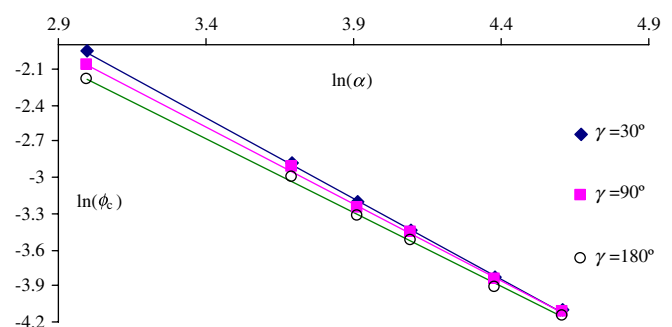**Fig. 13.** Critical fiber volume fraction varying with the fiber arm angle.

$$\sigma_e = \sigma_f (\phi - \phi_c)^t, \tag{18}$$

where σ_f is the electrical conductivity of the conductive phase, ϕ is the volume fraction of the conductive phase, ϕ_c is the critical volume fraction, and t is the conductivity exponent. It is postulated in this theory that t depends only on the space dimensionality and universality class of the problem. A universal value of $t = 1.3$ was proposed for 2-D materials, and $t = 2.0$ was suggested for 3-D materials [28,30]. In the current study, Eq. (18) together with $t = 2.0$ will be employed to calculate the electrical conductivity.

The effective electrical conductivity of the composite varying with the fiber volume fraction is graphically shown in Figs. 15 and 16. The numerical values illustrated in Figs. 15 and 16 are calculated using Eq. (18), with $t = 2.0$ and ϕ_c obtained in Section 3.4 for $\alpha = 12.5$ and 24 (see Fig. 13). It is seen from Figs. 15 and 16 that the composite conductivity is reduced as γ decreases (i.e., when the fiber becomes more curved). The same trend is observed for fibers with different aspect ratios, but the effect of γ on σ_e becomes less significant when α becomes large, as seen from Fig. 16, where $\alpha = 24$ as opposed to $\alpha = 12.5$ in Fig. 15. The effect of the fiber aspect ratio on the composite conductivity is further illustrated in Fig. 17. It is observed from Fig. 17 that the conductivity increases with α, which is more significant when α is small. Furthermore, the monotonic increase of the conductivity with the fiber volume fraction is clearly displayed in all curves shown in Figs. 15–17, which follows from the power-law relation in the percolation theory given in Eq. (18).

4. Summary

A 3-D Monte Carlo model for predicting electrical conductivity of polymer matrix composites filled with conductive curved fibers is presented. The new model accounts for the fiber curliness effect by using 3-D arm-shaped fibers, which are randomly distributed and oriented and have three adjustable parameters (i.e., the fiber arm length, the fiber aspect ratio, and the fiber arm angle). The

Fig. 12. Critical fiber volume fraction versus the fiber aspect ratio.

Fig. 14. Critical fiber volume fraction varying with the fiber aspect ratio.
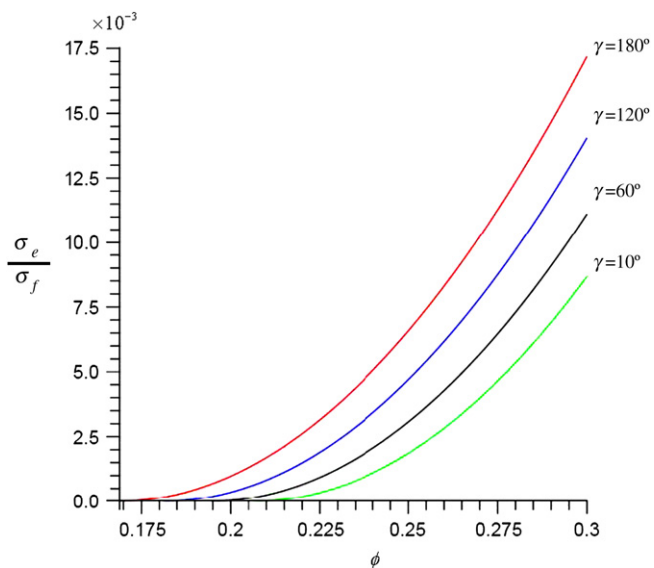
Fig. 15. Composite conductivity for fibers with different arm angles (with $\alpha = 12.5$).
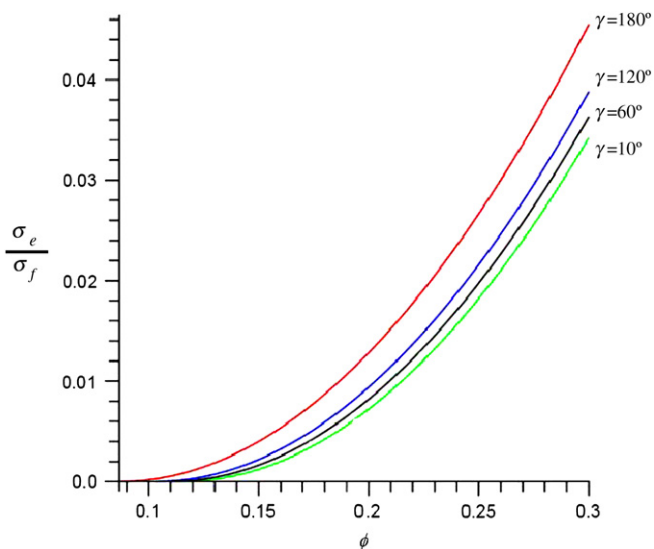

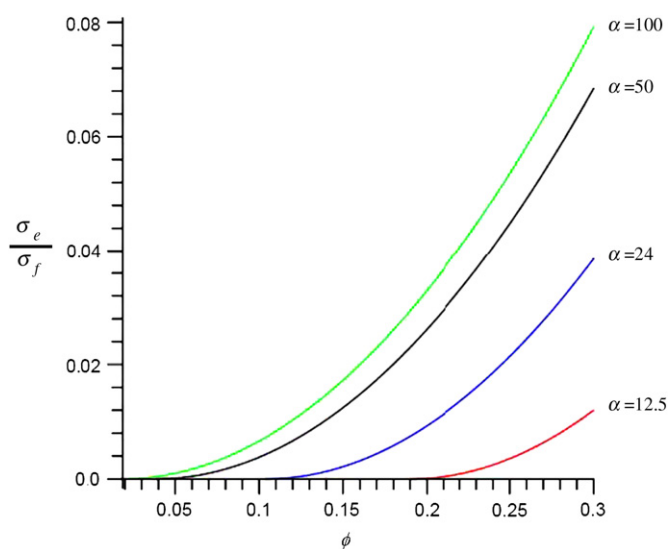**Fig. 16.** Composite conductivity for fibers with different arm angles (with $\alpha = 24$).

Fig. 17. Composite conductivity for fibers with different aspect ratios (with $\gamma = 90°$).

sample size and scaling effects are also considered in the current model.

The use of the Monte Carlo method leads to the determination of the percolation threshold, and the subsequent application of the percolation theory results in the prediction of the effective electrical conductivity of the composite.

The numerical results obtained using the newly developed model show that the fiber curliness has a large effect on the percolation behavior when the fiber aspect ratio is small: the less curved the fiber, the smaller the percolation threshold. The lowest value of the threshold is reached when the arm angle is 180° (i.e., straight fibers). However, this curliness effect becomes insignificant when the fiber aspect ratio is large. The current simulation results also reveal an exponential relationship between the aspect ratio and the percolation threshold: the higher the fiber aspect ratio, the lower the threshold. In addition, the effective electrical conductivity of the composite is found to decrease with the increase of the fiber curliness and with the decrease of the fiber aspect ratio. These newly obtained simulation results agree fairly well with experimental and numerical data published earlier by others.

Acknowledgments

Appendix A

Consider the ith and jth arm-shaped fibers in the system. Suppose that the central point (vertex) of the jth fiber is coincided with that of the ith fiber. Then it follows from Eqs. (8) and (9) that the distance between the centers of the ends of the ith and jth fibers, where $t = L$ and $s = L$, respectively, is

$$d = L\sqrt{2 + C_2}. \tag{A.1}$$

Next, consider the triangle formed by one end of the ith fiber (with $t = L$), one end of the jth fiber (with $s = L$) and the coincident central point of the two fibers. The distance between the centers of the two fiber ends, as the length of one side of the triangle, can be readily obtained as

$$d = 2L \sin\frac{\beta}{2}, \tag{A.2}$$

where β is the angle between the two equilateral sides of the triangle, with $0 \le \beta \le \pi$. Clearly, $\beta = 0$ or π if the ith and jth arm-shaped fibers are parallel to each other. A comparison of Eqs. (A.1) and (A.2) then gives

$$C_2 = -2 \cos^2\frac{\beta}{2}. \tag{A.3}$$

Therefore, $C_2^2 < 4$ for any $\beta \ne 0$. That is, $4 - C_2^2 > 0$ as long as the ith and jth arm-shaped fibers are not parallel to each other. This has proved the inequality used in Eq. (13b) for the case where the vertices of the two fibers coincide.

For the ith and jth arm-shaped fibers whose central points are separated by a distance d_o, the jth fiber can be moved by the distance d_o to have its vertex coincident with that of the ith fiber

without changing its orientation. As a result, the inequality proved above also holds for this more general case.

References

[1] Anderson SL. Random number generators on vector supercomputers and other advanced architectures. SIAM Rev 1990;32:221–51.
[2] Balberg I, Binenbaum N. Computer study of the percolation threshold in a two-dimensional anisotropic system of conducting sticks. Phys Rev B 1983;28:3799–812.
[3] Balberg I, Binenbaum N. Cluster structure and conductivity of three-dimensional continuum systems. Phys Rev A 1985;31:1222–5.
[4] Balberg I, Binenbaum N, Wagner N. Percolation thresholds in the three-dimensional sticks system. Phys Rev Lett 1984;52:1465–8.
[5] Bigg DM. Mechanical, thermal, and electrical properties of metal fiber-filled polymer composites. Polym Eng Sci 1979;19:1188–92.
[6] Boissonade J, Barreau F, Carmona F. The percolation of fibres with random orientations: a Monte Carlo study. J Phys A Math Gen 1983;16:2777–87.
[7] Bunde A, Dieterich W. Percolation in composites. J Electroceram 2000;5:81–92.
[8] Dalmas F, Dendievel R, Chazeau L, Cavaillé J-Y, Gauthier C. Carbon nanotube-filled polymer composites. Numerical simulation of electrical conductivity in three-dimensional entangled fibrous networks. Acta Mater 2006;54:2923–31.
[9] Dani A, Ogale AA. Electrical percolation behavior of short-fiber composites: experimental characterization and modeling. Compos Sci Technol 1996;56:911–20.
[10] Domany E, Kinzel W. Directed percolation in two dimensions: numerical analysis and an exact solution. Phys Rev Lett 1981;47:5–8.
[11] Essam JW. Percolation theory. Rep Prog Phys 1980;43:833–912.
[12] Foygel M, Morris RD, Anez D, French S, Sobolev VL. Theoretical and computational studies of carbon nanotube composites and suspensions: electrical and thermal conductivity. Phys Rev B 2005;71:104201.
[13] Hernandez YR, Gryson A, Blighe FM, Cadek M, Nicolosi V, Blau WJ, et al. Comparison of carbon nanotubes and nanodisks as percolative fillers in electrically conductive composites. Scripta Mater 2008;58:69–72.
[14] Kirkpatrick S. Percolation and conduction. Rev Mod Phys 1973;45:574–88.
[15] Hansen G. High aspect ratio sub-micron and nano-scale metal filaments. SAMPE J 2005;41:24–33.
[16] Lee YH, Kim HC. Three-dimensional electrical percolation behaviour in conductive short-fiber composites. J Mater Sci 1995;30:3033–6.
[17] Levinshtein ME, Shklovskii BI, Sur MS, Efros AL. The relation between the critical exponents of percolation theory. Sov Phys JETP 1976;42:197.
[18] Li C, Chou T-W. Continuum percolation of nanocomposites with fillers of arbitrary shapes. Appl Phys Lett 2007;90:174108.
[19] Li K, Gao X-L, Fielding JC, Benson Tolle T. Modeling of electrical conductivity of nickel nanostrand filled polymer matrix composites, J Comput Theor Nanosci, in press.
[20] Luo EZ, Ma JX, Xu JB, Wilson IH, Pakhomov AB, Yan X. Probing the conducting paths in a metal–insulator composite by conducting atomic force microscopy. J Phys D Appl Phys 1996;29:3169–72.
[21] McLachlan DS, Blaszkiewicz M, Newnham RE. Electrical resistivity of composites. J Am Ceram Soc 1990;73:2187–203.
[22] Moore C, Newman MEJ. Exact solution of site and bond percolation on small-world networks. Phys Rev E 2000;62:7059–64.
[23] Natsuki T, Endo M, Takahashi T. Percolation study of orientated short-fiber composites by a continuum model. Physica A 2005;352:498–508.
[24] Ogale AA, Wang SF. Simulation of the percolation behavior of quasi- and transversely isotropic short-fiber composites with a continuum model. Compos Sci Technol 1993;46:379–88.
[25] Ounaies Z, Park C, Wise KE, Siochi EJ, Harrison JS. Electrical properties of single wall carbon nanotube reinforced polyimide composites. Compos Sci Technol 2003;63:1637–46.
[26] Park SK, Miller KW. Random number generators: good ones are hard to find. Commun ACM 1988;31:1192–201.
[27] Pike GE, Seager CH. Percolation and conductivity: a computer study. I. Phys Rev B 1974;10:1421–34.
[28] Stauffer D. Introduction of percolation theory. London: Taylor & Francis; 1985.
[29] Taya M, Ueda N. Prediction of the in-plane electrical conductivity of a misoriented short fiber composite: fiber percolation model versus effective medium theory. ASME J Eng Mater Technol 1987;109:252–6.
[30] Toker D, Azulay D, Shimoni N, Balberg I, Millo O. Tunneling and percolation in metal–insulator composite materials. Phys Rev B 2003;68:041403(R).
[31] Yi YB, Berhan L, Sastry AM. Statistical geometry of random fibrous networks, revisited: waviness, dimensionality, and percolation. J Appl Phys 2004;96:1318–27.